Excitonic improvement of colloidal nanocrystals in salt powder matrix for quality lighting and color enrichment

Talha Erdem,[1,4] Zeliha Soran-Erdem,[1,4] Yusuf Kelestemur,[1] Nikolai Gaponik,[2] and Hilmi Volkan Demir[1,3,*]

[1]*Department of Electrical and Electronics Engineering, Department of Physics, and UNAM–Institute of Materials Science and Nanotechnology, Bilkent University, Ankara 06800, Turkey*
[2]*Physical Chemistry, TU Dresden, Bergstrasse 66b, D-01062 Dresden, Germany*
[3]*School of Electrical and Electronic Engineering, School of Physical and Mathematical Sciences, School of Materials Science and Engineering, Nanyang Technological University, Singapore 639798, Singapore*
[4]*These authors contributed equally.*
[*]*hvdemir@ntu.edu.sg*

Abstract: Here we report excitonic improvement in color-converting colloidal nanocrystal powders enabled by co-integrating nonpolar green- and red-emitting nanocrystal energy transfer pairs into a single LiCl salt matrix. This leads to nonradiative energy transfer (NRET) between the co-integrated nanocrystals in the host matrix. Here we systematically studied the resulting NRET process by varying donor and acceptor concentrations in the powders. We observed that NRET is a strong function of both of the nanocrystal concentrations and that NRET efficiency increases with increasing acceptor concentration. Nevertheless, with increasing donor concentration in the powders, NRET efficiency was found to first increase (up to a maximum level of 53.9%) but then to decrease. As a device demonstrator, we employed these NRET-improved nanocrystal powders as color-converters on blue light-emitting diodes (LEDs), with the resulting hybrid LED exhibiting a luminous efficiency >70 lm/W_{elect}. The proposed excitonic nanocrystal powders potentially hold great promise for quality lighting and color enrichment applications.

©2015 Optical Society of America

OCIS codes: (160.6000) Semiconductor materials; (250.5590) Quantum-well, -wire and -dot devices; (260.2160) Energy transfer; (230.3670) Light-emitting diodes; (230.0250) Optoelectronics.

References and links

1. T. Erdem and H. V. Demir, "Semiconductor nanocrystals as rare-earth alternatives," Nat. Photonics **5**(3), 126 (2011).
2. X. Michalet, F. F. Pinaud, L. A. Bentolila, J. M. Tsay, S. Doose, J. J. Li, G. Sundaresan, A. M. Wu, S. S. Gambhir, and S. Weiss, "Quantum dots for live cells, *in vivo* imaging, and diagnostics," Science **307**(5709), 538–544 (2005).
3. J. Y. Kim, O. Voznyy, D. Zhitomirsky, and E. H. Sargent, "25th anniversary article: Colloidal quantum dot materials and devices: A quarter-century of advances," Adv. Mater. **25**(36), 4986–5010 (2013).
4. E. Jang, S. Jun, H. Jang, J. Lim, B. Kim, and Y. Kim, "White-light-emitting diodes with quantum dot color converters for display backlights," Adv. Mater. **22**(28), 3076–3080 (2010).
5. T.-H. Kim, K.-S. Cho, E. K. Lee, S. J. Lee, J. Chae, J. W. Kim, D. H. Kim, J.-Y. Kwon, G. Amaratunga, S. Y. Lee, B. L. Choi, Y. Kuk, J. M. Kim, and K. Kim, "Full-colour quantum dot displays fabricated by transfer printing," Nat. Photonics **5**(3), 176–182 (2011).
6. V. Sukhovatkin, S. Hinds, L. Brzozowski, and E. H. Sargent, "Colloidal quantum-dot photodetectors exploiting multiexciton generation," Science **324**(5934), 1542–1544 (2009).
7. P. V. Kamat, "Quantum dot solar cells. Semiconductor nanocrystals as light harvesters," J. Phys. Chem. C **112**(48), 18737–18753 (2008).

#252027 Received 16 Oct 2015; accepted 21 Nov 2015; published 30 Nov 2015
© 2016 OSA

8. T. Erdem, S. Nizamoglu, X. W. Sun, and H. V. Demir, "A photometric investigation of ultra-efficient LEDs with high color rendering index and high luminous efficacy employing nanocrystal quantum dot luminophores," Opt. Express **18**(1), 340–347 (2010).
9. S. Nizamoglu, T. Erdem, X. W. Sun, and H. V. Demir, "Warm-white light-emitting diodes integrated with colloidal quantum dots for high luminous efficacy and color rendering," Opt. Lett. **35**(20), 3372–3374 (2010).
10. T. Erdem and H. V. Demir, "Color science of nanocrystal quantum dots for lighting and displays," Nanophotonics **2**(1), 57–81 (2013).
11. T. Erdem, Y. Kelestemur, Z. Soran-Erdem, Y. Ji, and H. V. Demir, "Energy-saving quality road lighting with colloidal quantum dot nanophosphors," Nanophotonics **3**(6), 373–381 (2014).
12. T. Otto, M. Müller, P. Mundra, V. Lesnyak, H. V. Demir, N. Gaponik, and A. Eychmüller, "Colloidal nanocrystals embedded in macrocrystals: Robustness, photostability, and color purity," Nano Lett. **12**(10), 5348–5354 (2012).
13. M. Müller, M. Kaiser, G. Stachowski, U. Resch-Genger, N. Gaponik, and A. Eychmüller, "Photoluminescence quantum yield and matrix-induced luminescence enhancement of colloidal quantum dots embedded in ionic crystals," Chem. Mater. **26**(10), 3231–3237 (2014).
14. T. Erdem, Z. Soran-Erdem, P. L. Hernandez-Martinez, V. K. Sharma, H. Akcali, I. Akcali, N. Gaponik, A. Eychmüller, and H. V. Demir, "Sweet plasmonics: sucrose macrocrystals of metal nanoparticles," Nano Res. **8**(3), 860–869 (2015).
15. Z. Soran-Erdem, T. Erdem, P. L. Hernandez-Martinez, M. Z. Akgul, N. Gaponik, and H. V. Demir, "Macrocrystals of colloidal quantum dots in anthracene: exciton transfer and polarized emission," J. Phys. Chem. Lett. **6**(9), 1767–1772 (2015).
16. T. Erdem, Z. Soran-Erdem, V. K. Sharma, Y. Kelestemur, M. Adam, N. Gaponik, and H. V. Demir, "Stable and efficient colour enrichment powders of nonpolar nanocrystals in LiCl," Nanoscale **7**(42), 17611–17616 (2015).
17. T. Erdem, S. Nizamoglu, and H. V. Demir, "Computational study of power conversion and luminous efficiency performance for semiconductor quantum dot nanophosphors on light-emitting diodes," Opt. Express **20**(3), 3275–3295 (2012).
18. P. Zhong, G. He, and M. Zhang, "Optimal spectra of white light-emitting diodes using quantum dot nanophosphors," Opt. Express **20**(8), 9122–9134 (2012).
19. W. K. Bae, K. Char, H. Hur, and S. Lee, "Single-step synthesis of quantum dots with chemical composition gradients," Chem. Mater. **20**(2), 531–539 (2008).
20. O. Chen, J. Zhao, V. P. Chauhan, J. Cui, C. Wong, D. K. Harris, H. Wei, H.-S. Han, D. Fukumura, R. K. Jain, and M. G. Bawendi, "Compact high-quality CdSe-CdS core-shell nanocrystals with narrow emission linewidths and suppressed blinking," Nat. Mater. **12**(5), 445–451 (2013).
21. K. H. Ibnaouf, S. Prasad, M. S. Al Salhi, A. Hamdan, M. B. Zaman, and L. El Mir, "Influence of the solvent environments on the spectral features of CdSe quantum dots with and without ZnS shell," J. Lumin. **149**, 369–373 (2014).
22. R. Koeppe and N. S. Sariciftci, "Photoinduced charge and energy transfer involving fullerene derivatives," Photochem. Photobiol. Sci. **5**(12), 1122–1131 (2006).
23. S. Nizamoglu, E. Sari, J.-H. Baek, I.-H. Lee, and H. V. Demir, "Nonradiative resonance energy transfer directed from colloidal CdSe/ZnS quantum dots to epitaxial InGaN/GaN quantum wells for solar cells," Phys. Status Solidi Rapid Res. Lett. **4**(7), 178–180 (2010).

1. Introduction

Semiconductor colloidal nanocrystals, which offer favorable and unique optical properties such as narrow and tunable emission, broad absorption, and high quantum efficiencies [1], have been in the center of interest in numerous fields from biology [2] to photonics [3]. After twenty years of their first colloidal synthesis, today these materials are utilized in various applications including displays [4,5], sensors [6], solar-cells [7], and illuminants for general [8–10] and outdoor lighting [11]. Their main Achille's heel is the problems associated with their deterioration occurring due to their moderate stability as well as limited compatibility with the encapsulants and fabrication techniques.

One of the remedies to these problems is the incorporation of nanocrystals into crystalline host matrices of ionic salts as it has been proposed by Otto et al. [12]. The effect of this crystallization process was on the quantum efficiency was studied by Müller et al. and efficiencies of crystals above the in-dispersion efficiencies were reported [13]. Subsequently, we investigated the plasmonic interaction between nanocrystals and gold nanoparticles within sucrose macrocrystals and reported an improvement of 58% in the quantum efficiency via plasmonic interplay [14]. In these works, however, the host matrix of nanocrystals allows for the incorporation of the nanocrystals dispersed only in water. Therefore, the types and performance of the applicable nanocrystals are strongly limited.

#252027 Received 16 Oct 2015; accepted 21 Nov 2015; published 30 Nov 2015
© 2016 OSA

To resolve these handicaps, Soran-Erdem et al. embedded the oleic acid capped nanocrystals into the anthracene matrix, which is a blue-emitting crystalline organic semiconductor material soluble in chloroform [15]. However, the quantum efficiency of the nanocrystals in this material system decreased and the thermal stability of the nanocrystals in anthracene is limited due to the low thermal stability of anthracene. As an alternative to organic crystals, our group developed a vacuum-assisted technique for incorporating nanocrystals in nonpolar solvents into LiCl salt without phase transfer. With this technique we significantly improved the emission stability of the nanocrystals and protected their in-solution quantum efficiencies in salt matrix [16].

Since the distance between the nanocrystals embedded into LiCl matrix can be as low as 10 nm [16], this material system can be a good candidate for utilizing nonradiative energy transfer (NRET) in color enrichment films. With the small distance between the nanocrystals allowing for dipole-dipole coupling, high NRET efficiencies can be realized within these powders as opposed to our previous work [15] where low quantum efficiency of anthracene restricted the efficiency of NRET to red-emitting nanocrystals below 30%. Furthermore, the broad emission spectrum of anthracene, which always exists in the photoluminescence of the macrocrystal, did not allow for fine-tuning the final emission spectrum. This is, however, an important requirement for general lighting and display applications [10].

Since the utilization of only nanocrystals within powders can easily help to control the spectral features of the color converting materials [17,18], here we aim at developing and demonstrating a material system consisting of dielectric salt encapsulating nanocrystals that undergo NRET among them. For this purpose, here we co-integrated green- and red-emitting nanocrystals into a single LiCl salt matrix for the first time and studied the NRET dynamics between these nanocrystals within the salt powder. We systematically varied the green-emitting nanocrystals as the exciton donors to red-emitting nanocrystals as the exciton acceptors by controlling their incorporation amounts. In our experiments, we achieved a maximum NRET efficiency of 53.9%, which is almost twice the value that could be previously obtained in anthracene macrocrystal hosts. Furthermore, we employed these nanocrystal powders on a proof-of-concept light-emitting diode as color conversion film and obtained a high luminous efficiency of 70 lm/W_{elect}. We believe that this present study can possibly pave the way for a wide-spread use of LiCl encapsulation of colloidal nanocrystals on light-emitting diodes for use as robust, efficient phosphor powders compatible with the packaging capabilities of the lighting industry.

2. Experimental methods

2.1 Chemicals

Cadmium oxide (CdO, 99.99%), zinc acetate ($Zn(acetate)_2$, 99.9%), sulfur (S, 99.9%), selenium (Se, 99.99%) and lithium chloride (LiCl) were purchased from Sigma-Aldrich in powder form. Oleic acid (OA, 90%), trioctylphosphine (TOP, 90%), 1-octadecene (1-ODE, 90%), dodecanethiol (DDT, 99%), octanethiol, cadmium oleate, tetrahydrofuran (THF) and hexane were bought from Sigma-Aldrich and used without any purification.

2.2 Synthesis of colloidal nanocrystals

Colloidal nanocrystals having peak emission wavelengths of 534 nm (green) and 604 nm (red) were synthesized to be used in this study as exciton-donating and exction-accepting nanocrystals, respectively. The details of their syntheses were explained below.

2.2.1 Synthesis of green-emitting CdSe/CdZnSeS/ZnS colloidal nanocrystals

For a typical synthesis of CdSe/CdZnSeS/ZnS nanocrystals, we followed the method published by Bae et al. [19]. Briefly, 0.4 mmol of CdO, 4 mmol of $Zn(acetate)_2$, 5.6 mL of OA and 20 mL of 1-ODE were loaded into a 50 mL three-neck flask. Then, the mixture was

#252027 Received 16 Oct 2015; accepted 21 Nov 2015; published 30 Nov 2015
© 2016 OSA

degassed for 2 h at 100 °C under vigorous stirring and the temperature of mixture was raised to 310 °C under argon flow. At this temperature, 0.1 mmol of Se powder and 4 mmol of S powder both dissolved in 3 mL of TOP were quickly injected into the reaction flask. Following 10 min of growth, the mixture was cooled down to room temperature and precipitated with hexane/acetone mixture. Finally, the resulting nanocrystals were dissolved in hexane and used for further experiments.

2.2.2 Synthesis of red-emitting CdSe/CdS core/shell colloidal nanocrystals

The synthesis of CdSe/CdS core/shell nanocrystals was carried out following the method reported in Chen et al [20]. For the synthesis of CdSe core, cadmium myristate and selenium dioxide were used as cadmium and selenium precursors, respectively. These chemicals were dissolved in octadecene and evacuated at room temperature for 10-15 minutes. Subsequently, the solution was heated to 240 °C within 10 min. Then, the temperature of the solution was kept at 240 °C for the growth of CdSe cores until the desired size of CdSe cores was obtained. After the reaction was stopped by decreasing the temperature, as-synthesized CdSe cores were precipitated by using acetone and dissolved in hexane. In the second step, CdSe cores were coated with CdS shell. For this purpose, certain amount of CdSe cores (100 nmol) dissolved in hexane was loaded to four-neck flask containing 3 mL octadecene and 3 mL oleylamine. After the solution was degassed at 100 °C in order to remove hexane and any other organic residuals, the temperature of the reaction was set to 300 °C for the coating of CdS shell under argon atmosphere. When the temperature reached 240 °C, calculated amounts of cadmium and S precursors corresponding to six monolayers of CdS were injected with a rate of 3 mL/min. After the injection of shell precursors were completed within two hours at 300 °C, the reaction was stopped and the temperature was decreased to room temperature. As-synthesized CdSe/CdS core/shell nanocrystals were precipitated with acetone and dispersed in hexane.

2.3 Preparation of the LiCl encapsulated nanocrystal powders, films, and light-emitting diode

For the preparation of oversaturated LiCl stock solution, 1.83 g of LiCl was dissolved in 50 mL of tetrahydrofuran (THF) in a glovebox with nitrogen environment. Prior to the encapsulation of the nanocrystals in LiCl, the green- and red-emitting nanocrystal concentrations were set to 3.7 mg/mL. Subsequently, hexane of only green- and only red-emitting nanocrystals along with that of their mixtures were evaporated. The volumes of the nanocrystals used in this work were listed below in Table 1. After drying the solvent, nanocrystals were dispersed in 250 μL of THF and 1 mL of LiCl stock solution (36.6 mg) was slowly added. Subsequently, samples were placed within a desiccator to encapsulate the nanocrystals within LiCl powders by completely evaporating THF.

Table 1. The volumes for green- (donor) and red-emitting (acceptor) nanocrystals used for incorporation into LiCl.

	Green (Donor)				Red (Acceptor)		
Volume	25 μL	50 μL	75 μL	100 μL	50 μL	150 μL	250 μL

The nanocrystal incorporated LiCl powder films were prepared by mixing ~6.3 mg of the powders with a commercial two-component epoxy (Bison). Similarly, the light-emitting diode was prepared by integrating 23 mg of the 50 μL green (donor) and 250 μL red-emitting (acceptor) on an Avago ASMT blue LED using Bison epoxy.

2.4 Optical Characterizations

Steady-state photoluminescence spectra of nanocrystal dispersion and nanocrystal incorporated LiCl films were taken using an Ocean Optics Maya 2000 spectrometer equipped with a Hamamatsu integrating sphere, a Spectral Products monochromator at an excitation wavelength of 460 nm and a Xenon lamp as the excitation source.

#252027 Received 16 Oct 2015; accepted 21 Nov 2015; published 30 Nov 2015
© 2016 OSA

Absorption spectra of green-emitting and red-emitting nanocrystal solutions were taken using Carry 100 UV-Vis spectrometer. However, the absorption spectrum of the nanocrystal embedded LiCl powders could not be measured reliably due to the scattering problem,.

The photoluminescence lifetimes of the films were taken using a PicoHarp 200 time-resolved single photon counting system (PicoQuant). A pulsed laser emitting at 375 nm was employed as the excitation source. Three exponentials were fitted to the decay curves and amplitude averaged lifetimes were reported as the lifetime.

3. Results and discussion

In this work, we have investigated for the first time the nonradiative energy transfer from green to red nanocrystals that are immobilized within a salt matrix. Here we benefitted from the solubility of LiCl in THF which simultaneously can disperse nanocrystals as well. This enabled the incorporation of the nonpolar nanocrystals into LiCl salt without any ligand exchange. Furthermore, this vacuum assisted salt incorporation of nanocrystals allowed for immobilizing the nanocrystals emitting different colors in close proximity so that nonradiative energy transfer (NRET) can take place.

Toward this aim, we have synthesized green-emitting alloyed core/shell nanocrystals of CdSe/CdZnSeS/ZnS according to Bae et al. [19] and red-emitting CdSe/CdS core/shell nanocrystals according to Chen et al. [20] These as-synthesized nanocrystals exhibited emission peaks at 534 nm and 604 nm, respectively. We note that there is a strong overlap between the emission spectrum of the green-emitting nanocrystals and absorption spectrum of the red-emitting nanocrystals as presented in Fig. 1. This suggests that NRET is possible from the green-emitting nanocrystals to the red-emitting nanocrystals via dipole-dipole interaction if these nanocrystals are placed in close proximity. Because the distance between nanocrystals can be below 10 nm when they are embedded in LiCl using the technique presented in Ref [16], NRET from green-emitting nanocrystals to red-emitting nanocrystals becomes possible. Therefore, in this work we embedded these nanocrystals into LiCl matrix in varying amounts as shown in Table 1. The amount of the nanocrystals embedded into powders was calculated by dissolving a certain amount of powders in THF, measuring the absorption spectra of the nanocrystals, and comparing the absorbance of the nanocrystals in the dissolved powders with the absorbance of the nanocrystal dispersion. The results showed that almost all the nanocrystals used were incorporated into LiCl matrix. The estimated molar concentrations calculated according to Ref [16]. then became ~2.68-3.82 pmol/mg, ~5.36-7.64 pmol/mg, ~8.04-11.5 pmol/mg, and ~10.7-15.3 pmol/mg for the powders prepared using 25, 50, 75, and 100 μL of nanocrystals, respectively. A similar calculation of the red-emitting nanocrystal powders yielded ~8.92-10.7 pmol/mg, ~26.8-32.1 pmol/mg, and ~44.6-53.5 pmol/mg for 50, 150, and 250 μL of nanocrystals, respectively. To obtain exction-transfeering nanocrystal embedded LiCl powders, we hybridized these green and red-emitting nanocrystals with the designated amounts stated above prior to their incorporation into LiCl and subsequently carried out the incorporation into salt. In this material system, green nanocrystals act as exciton donors while red nanocrystals serve as exciton acceptors. To assist the reader, we have chosen to use the volumes of the incorporated nanocrystals instead of their weights or molar concentrations throughout the rest of the manuscript.

#252027 Received 16 Oct 2015; accepted 21 Nov 2015; published 30 Nov 2015
© 2016 OSA

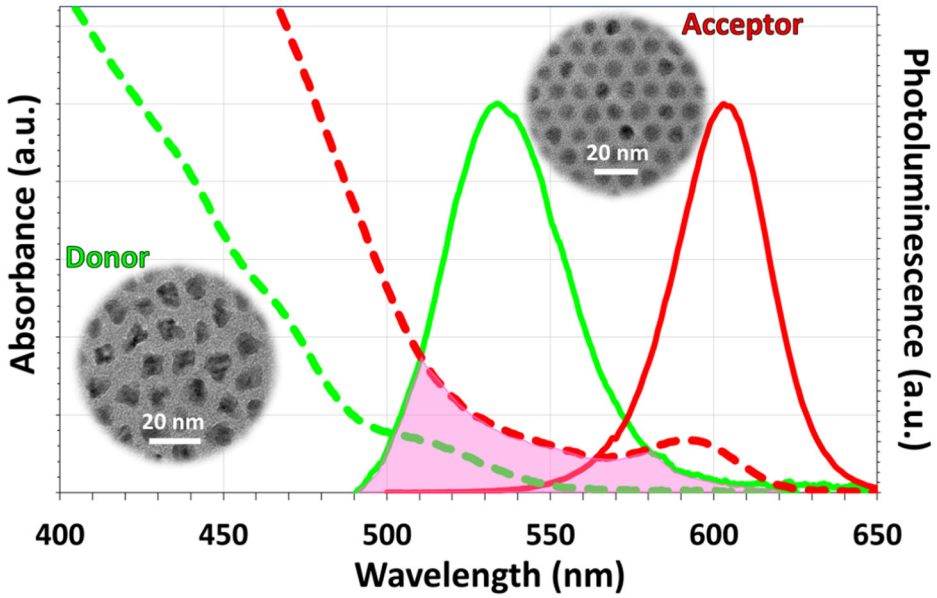


Fig. 1. Photoluminescence spectra of the green-emitting donor and red-emitting acceptor nanocrystals (shown with green and red continuous lines, respectively) and their absorption spectra (shown with green and red dashed lines, respectively). In the inset, we provide the transmission electron microscopy images of these nanocrystals.

Within the framework of our study, we first investigated the photoluminescence of the nanocrystal incorporated powders (Fig. 2). In the powders with only single color nanocrystal incorporation, we observe a red-shift of 2 and 8 nm for green and red nanocrystals in LiCl powders compared to their dispersions, respectively. In addition, we did not observe an apparent red-shift in the emission spectra of the nanocrystals with the increasing nanocrystal incorporation amount. If the aggregation of nanocrystals were prominent, however, we would expect increasing red-shift of nanocrystal emission with increasing nanocrystal incorporation amount. This shows that the red-shift in the emission spectrum is mainly caused by the interaction of the dipoles in the nanocrystals with the surrounding medium [21]. Another observation is the decreasing intensity of the green-emitting nanocrystals when red-emitting nanocrystals are co-immobilized within LiCl powders. In parallel to this, we observe an increase in the intensity of the red nanocrystals when hybridized with green nanocrystals compared to the intensity of the only red nanocrystals immobilized in LiCl powders.

In these hybrid powders, the decrease of the green-emitting nanocrystal intensity along with the increase of the red-emitting nanocrystal intensity can be explained by both the radiative and nonradiative energy transfer. Radiative energy transfer can occur via the absorption of the green light by the red nanocrystals; as a result, the intensity of the green light decreases while the red intensity increases. This process does not require close proximity between the nanocrystals; instead, it only requires the emitted green light to reach the red-emitting nanocrystals that absorb the green light. On the other hand, NRET requires close proximity between green and red nanocrystals within LiCl to transfer the excitons from one emitter to another. These two energy transfer mechanisms can be safely distinguished by time-resolved fluorescence (TRF) spectroscopy. While the radiative energy transfer does not have any effect on the time-resolved decay of the emitter, the occurrence of the NRET can be monitored in the TRF decay of the donor as a fastened decay curve. In addition, slowed-down acceptor decay curves are also expected if the lifetime of the acceptor is comparable to that of the donor lifetime [22]. Since in our system we utilize nanocrystals having similar lifetimes,

#252027 Received 16 Oct 2015; accepted 21 Nov 2015; published 30 Nov 2015
© 2016 OSA

we expect to observe an increase in the red nanocrystal lifetime simultaneous to decreasing lifetime of the green-emitting donor nanocrystals.

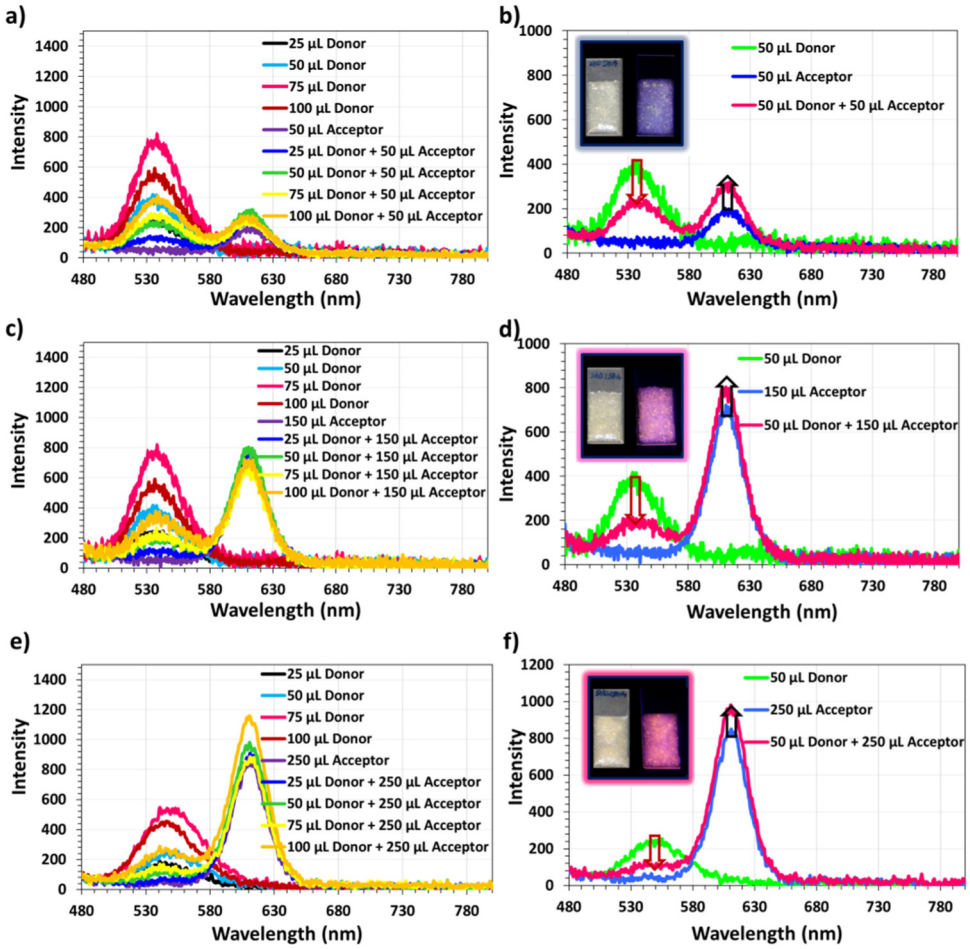


Fig. 2. Photoluminescence spectra of the films prepared using green-red nanocrystal hybrids embedded into LiCl powders. Here, the green nanocrystals serve as exciton donors while the red nanocrystals accept excitons. In (a), (c), and (e) the spectra of the only green nanocrystal embedded powders are given together with the hybrid and only red-emitting acceptor nanocrystal embedded powders prepared using 50, 150, and 250 µL of nanocrystals, respectively. Frames (b), (d), and (f) show the variation of the spectra for the cases where 50 µL of green (donor) nanocrystals are embedded into LiCl together with 50, 150, and 250 µL of acceptor, respectively. The inset images are the real color photographs of these films under ambient (left) and UV lighting (right).

To reveal the emission mechanisms within the LiCl powders incorporating green and red nanocrystals, we measured the TRF decays of the films. In Fig. 3, we present exemplary decay curves of the hybrid LiCl films prepared using powders incorporating 250 µL of red-emitting nanocrystals together with 25-100 µL of green-emitting nanocrystals; however, similar trends are observed in the samples prepared by incorporating 50 and 150 µL of red nanocrystals. All of these data indicate a clear acceleration in the time-resolved decay curve of the green nanocrystals in LiCl powders when co-immobilized in LiCl together with red-emitting nanocrystals; while slowed down acceptor decays follow. These observations confirm that NRET takes place between green-emiting nanocrystals and red-emitting nanocrystals.

#252027 Received 16 Oct 2015; accepted 21 Nov 2015; published 30 Nov 2015
© 2016 OSA

To quantitatively analyze the NRET dynamics within the hybrid powders, we fitted the TRF decays with three exponential functions and calculated the amplitude averaged lifetimes. Subsequently, the efficiency of the NRET process is calculated according to Eq. (1) where τ_D stands for the donor lifetime in the absence of the acceptor while τ_{DA} stands for the donor lifetime in the presence of acceptor. These calculated lifetimes are illustrated below in Fig. 4.

$$\eta = 1 - \frac{1/\tau_D}{1/\tau_{DA}}. \quad (1)$$

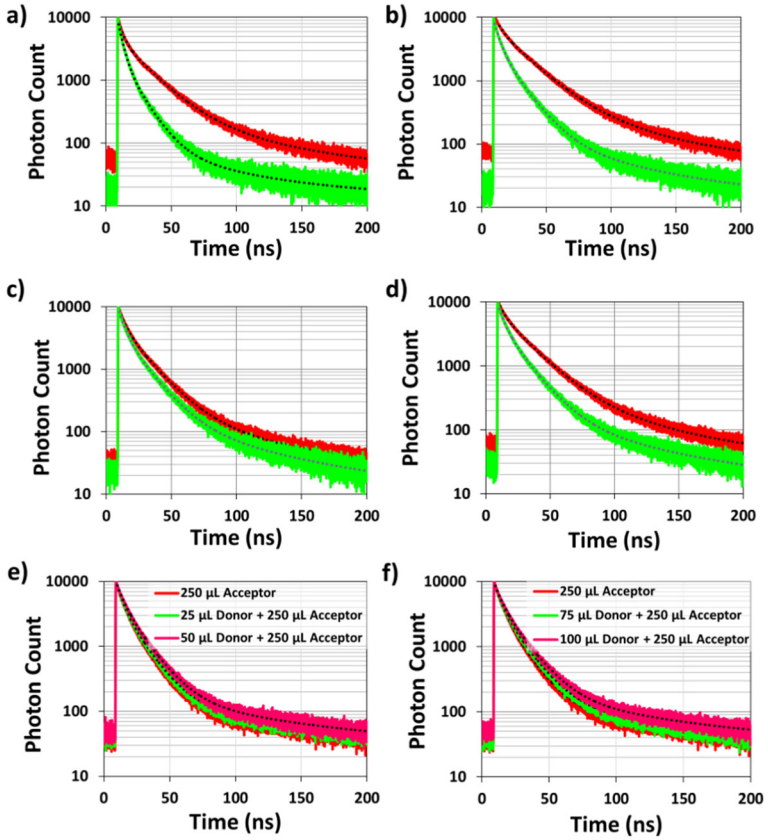


Fig. 3. Time-resolved fluorescence decays of green-emitting exciton-donating nanocrystals within powders prepared using (a) 25 µL donor nanocrystals (red line) and hybrid of 25 µL donor nanocrystals together with 250 µL red-emitting exciton-accepting nanocrystals (green line), (b) 50 µL donor nanocrystals (red line) and hybrid of 50 µL donor nanocrystals together with 250 µL acceptor nanocrystals (green line), (c) 75 µL donor nanocrystals (red line) and hybrid of 75 µL donor nanocrystals together with 250 µL acceptor nanocrystals (green line), and (d) 100 µL donor nanocrystals (red line) and hybrid of 100 µL donor nanocrystals together with 250 µL acceptor nanocrystals (green line) at the donor emission peaks. Frames (e) and (f) show the TRF decays of the acceptor nanocrystals alone and in hybrid nanocrystal powders. The black dashed lines are the fitted multiexponential functions on the TRF decays.

In this figure, we observe that the lifetimes of the green nanocrystals decrease when they are hybridized with the red nanocrystals in LiCl compared to the case of only green nanocrystals embedded within LiCl for all the red nanocrystal amounts in the hybrid powders. For example, the lifetime of the green nanocrystals decreases from 21.0 ns to 9.7 ns when 50 µL green nanocrystals are embedded into LiCl together with 250 µL of red nanocrystals. In addition, the red-nanocrystals exhibit a lengthened lifetime in hybrid powders. For instance,

#252027 Received 16 Oct 2015; accepted 21 Nov 2015; published 30 Nov 2015
© 2016 OSA

the lifetime of the red-nanocrystals increases from 10.0 ns to 12.0 ns following the hybridization of 250 µL red nanocrystals with 50 µL of green nanocrystals in LiCl. These findings show that excitons are donated by green-emitting nanocrystals to red-emitting nanocrystals. It is here worth noting that NRET in such material system might originate from dipole-dipole interaction or charge transfer. However, in our system the high energy barrier occurring due to the LiCl in the medium and ZnS shell of the green nanocrystals blocks the charge transfer [23]. This hypothesis is also supported by the lengthened acceptor lifetimes which should have shortened if charge transfer occurred between the nanocrystals [22]. Therefore, here we conclude that the main NRET mechanism taking place in our system is Förster like energy transfer that relies on the dipole-dipole interaction of two emitters.

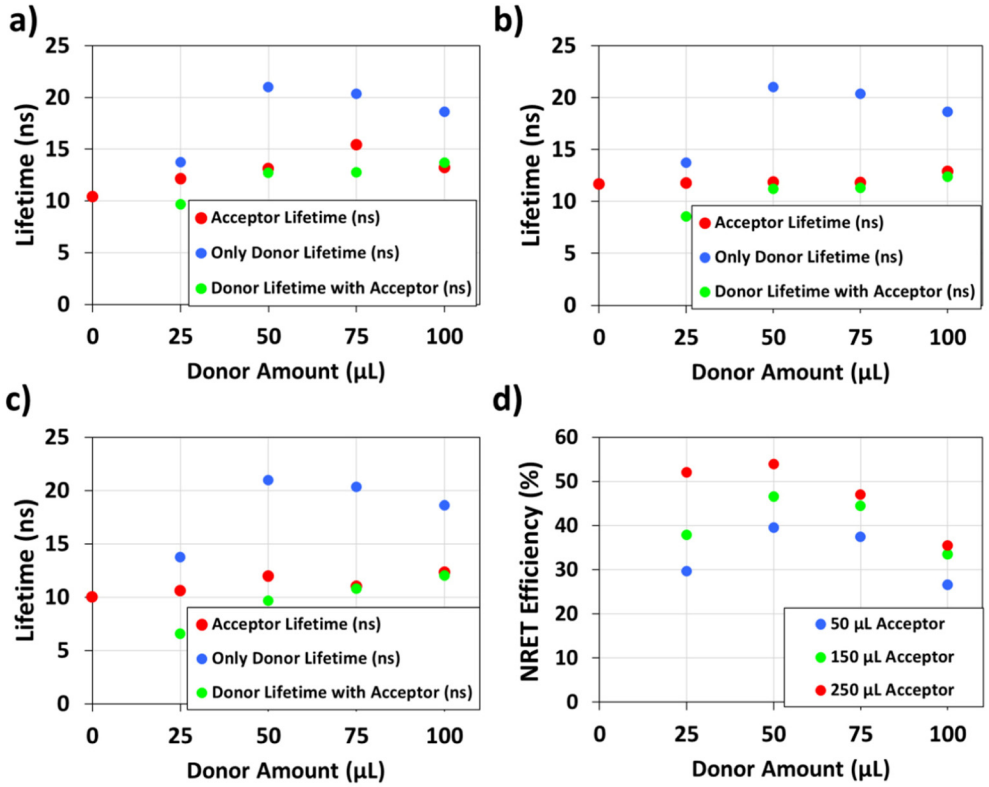


Fig. 4. Amplitude averaged lifetimes of only donor nanocrystal embedded LiCl powders, only acceptor nanocrystal embedded LiCl powders, and powders prepared using donor and acceptor nanocrystals. Frame (a) presents the lifetimes for the incorporated acceptor amount of 50 µL while in (b) and (c) the illustrated lifetimes stand for the powders prepared using 150 and 250 µL of acceptor, respectively. Frame (d) presents the NRET efficiency of the hybrid nanocrystal powders for varying acceptor incorporation amounts.

The NRET efficiencies presented in Fig. 4(d) exhibit a dependence on the amounts of the incorporated exciton donating green nanocrystals and exciton accepting red nanocrystals. As expected, as the amount of the acceptor nanocrystals increases, the efficiency of the NRET process increases for all the donor amounts. This is because the number of acceptors surrounding the donor nanocrystals increases; as a result, the probability of exciton transfer from the donor nanocrystals to acceptor nanocrystals increases leading to increased NRET efficiencies. On the other hand, for the fixed incorporated acceptor amounts the NRET efficiency first increases with the increasing donor amount in the powders up to 39.6%, 46.6%, and 53.9% in the samples prepared by mixing 50 µL of green-emitting donor nanocrystals with 50, 150, and 250 µL of red-emitting nanocrystals, respectively.

#252027 Received 16 Oct 2015; accepted 21 Nov 2015; published 30 Nov 2015
© 2016 OSA

Nevertheless, further increase of the donor concentration in the powders is found to decrease the NRET efficiency. This observation can be explained with two effects that possibly work together. The first one is that there is enough acceptor in the close proximity of the donors to transfer their excitons up to a donor concentration around ~5.36-7.64 pmol/mg (50 µL); but beyond this concentration a competition starts to occur between the donor nanocrystals to transfer their excitons. As a result, some excitons can be transferred nonradiatively while some of them cannot as the donor concentration in the powders further increases. Consequently, the lifetime of the donor nanocrystals in the nanocrystal hybrid powders converges to the lifetime of the only green nanocrystal incorporated powders with further increase of donor nanocrystal concentration. The second effect is that after a certain point increasing the donor concentration cannot increase the number of donors which are in close proximity of the acceptors. As a result, the number of the nanocrystals transferring their excitons cannot increase. In this case, further addition of donors would decrease the fraction of the donors undergoing exciton transfer. Consequently, the donor lifetime in the hybrid nanocrystal powders starts to converge to the lifetime of the only green nanocrystal embedded LiCl powders leading to smaller ensemble NRET efficiencies.

This material system of nanocrystal embedded LiCl powders is an excellent system for use on light-emitting devices as color converters because it offers high-efficiency along with the improved stability of nanocrystals [16] and compatibility with the current production facilities of the light-emitting diode (LED) producers. In this work, we also utilized NRET in these powders to realize exciton transferring light-emitting diodes. For this purpose, we integrated about 23 mg of the powders prepared using 50 µL of green and 250 µL of red nanocrystals, which achieved the highest NRET efficiency among our samples, on a blue LED emitting at 460 nm. This LED, whose emission spectrum is presented in Fig. 5, reached a luminous efficiency above 70 lm/W_{elect} in the violet-purple color regime with chromaticity points around x = 0.32-0.35 and y = 0.23-0.26. Considering this performance, we believe that this NRET improved LEDs can be a good alternative for replacing violet LEDs based on epitaxially grown GaN.

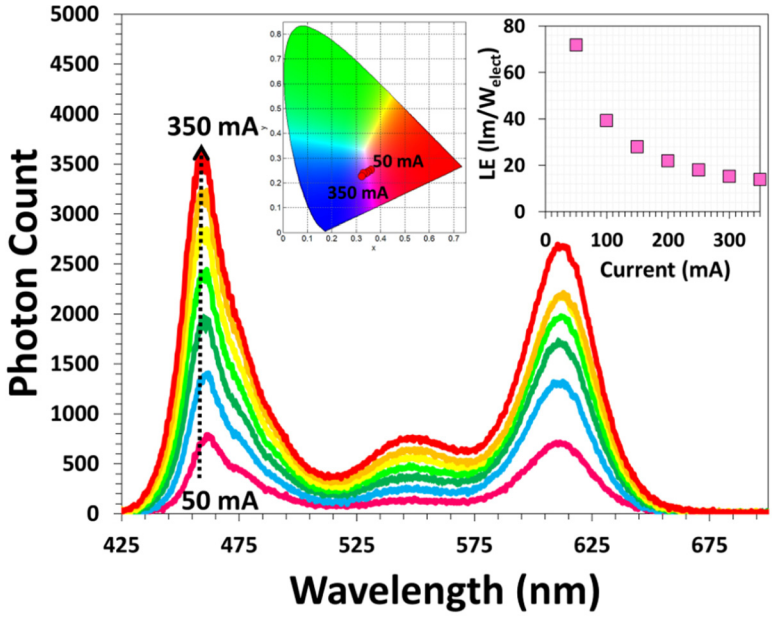


Fig. 5. Emission spectrum of the NRET enhanced nanocrystal embedded LiCl powders at varying currents together with the chromaticity points of the emitted light (inset, left) and luminous efficiency of the device (LE) (inset, right).

#252027 Received 16 Oct 2015; accepted 21 Nov 2015; published 30 Nov 2015
© 2016 OSA

4. Conclusions

In conclusion, here we co-immobilized nonpolar green and red-emitting nanocrystals into LiCl salt matrix. The short distance between these co-integrated nanocrystals allowed the green-emitting ones to strongly transfer their excitons to the red-emitting ones. For a systematic study, we varied the concentrations of the donor and acceptor nanocrystals within these powders and studied the NRET efficiency. We observed that the increase of the acceptor incorporation in the powders increases the NRET efficiency because there are more acceptors to receive excitons per donor. On the other hand, the increasing donor concentration in the powders was found first to increase the energy transfer efficiency and then to decrease it, which is attributed to the competition between the donors with increasing donor concentration and to the increased amount of donors immobilized further away from the acceptors. In our powder system, the NRET efficiency reached a maximum level of 53.9% at the donor concentration of ~5.36-7.64 pmol/mg and the acceptor concentration of ~44.6-53.5 pmol/mg. Subsequent to these analyses, we integrated these NRET-enhanced color-converting nanocrystal powders on blue LEDs. The resulting violet-emitting LED reached a luminous efficiency above 70 lm/W_{elect}. We believe that these excitonic LiCl powders of colloidal nanocrystals, which offer improved stability, robustness, and compatibility to current packaging facilities of the LED industry, can find wide-spread use in lighting and display applications.

Acknowledgements

We acknowledge ESF EURYI, EU-FP7 Nanophotonics4Energy NoE, BMBF TUR 09/001, and TUBITAK EEEAG 109E002, 109E004, 110E010, 110E217, 112E183 and in part by NRF-CRP-6-2010-02 and NRF-RF-2009-09. H.V.D. acknowledges additional support from TUBA-GEBIP, T.E. and Y.K. acknowledge support from TUBITAK BIDEB.

#252027 Received 16 Oct 2015; accepted 21 Nov 2015; published 30 Nov 2015
© 2016 OSA